Real-Time Observation of Fiber Network Formation in Molecular Organogel: Supersaturation-Dependent Microstructure and Its Related Rheological Property

Rongyao Wang, Xiang-Yang Liu,* Junying Xiong, and Jingliang Li

Biophysics and Micro/nanostructures Lab, Department of Physics, Blk. S12, National University of Singapore, 2 Science Drive 3, Singapore 117542

Received: August 12, 2005; In Final Form: February 8, 2006

Low-molecular mass organic gelators self-organizing into three-dimensional fiber networks within organic solvents have attracted much attention in recent years. However, to date, how the microstructure of fiber network is formed in a gelation process and the key factors that govern the topological structure of a gel network remain to be determined. In this work, we address these issues by investigating the in situ formation of the gel networks in the *N*-lauroyl-L-glutamic acid di-*n*-butylamide (GP-1)/propylene glycol (PG) system. By using optical microscopy, the time evolution of the gel network microstructure was investigated under various supersaturation conditions. It is found that supersaturation is one of the key factors that govern the topological structure of a gel network. In particular, the creation of the junctions turns out to be supersaturation-dependent. The rheological experiments further revealed the correlation between topological structure and mechanical properties. It suggests that the rheological properties can be effectively modified by tuning the microstructure topology of the gel network. Our results reported here provide new physical insight into the formation kinetics of a molecular gel. Furthermore, this work could be important in constructing and engineering a supramolecular structure for the purpose of applications.

1. Introduction

Low-molecular mass organic gelators (LMOGs) capable of immobilizing various organic solvents have been the subject of rapidly growing interest in recent years, because of their potential applications in the food industry, drug manufacturing, cosmetics, etc.[1−4] The LMOG gels are viscoelastic solidlike materials, possessing both the elastic properties of ideal solids and the viscous properties of Newtonian liquids. The three-dimensional fiber networks are the substantial component of a self-supporting gel that entraps large amounts of organic solvent, principally through capillary force or surface tension, and the junctions, i.e., the nodes of the fiber network, provide rigidity to the microstructure. So far, several imaging techniques such as SEM,[1,5] TEM,[6,7] AFM,[8,9] and optical microscopy[10,11] have been used to investigate the gel network structure at either nanometer or micrometer resolution. These images show that the three-dimensional fiber network usually consists of fiber branches, fiber bundles, and/or fiber entanglements, and the density, thickness, and length of fibers can be significantly different from one gel system to another. However, how the fiber network is formed in a gelation process and, in particular, how the junctions are created during the development of a gel network remain unclear.

To address these issues, an in situ investigation of gel network structure formation is necessary. Several techniques such as light scattering[12] and neutron scattering,[13] various spectroscopic techniques,[13] and rheology[13,14] are able to probe the different stages of the gelation process ranging from the initial aggregation to the development of the network, but the real-time observation of the evolution of a fiber network has rarely been reported,[8,11] due to the limitations arising from the imaging techniques themselves. For instance, SEM and TEM cannot be used to conduct the in situ analysis due to the requirement of high vacuum. AFM can be used in an ambient environment but is limited by its invasive measurement. For example, when the sample is exposed to ambience, the evaporation of solvent may exert a significantly negative influence on gel formation. Comparatively, optical microscopy can serve as an attractive tool for the in situ monitoring of the gelation process due to its advantages of noninvasive detection and accessibility to a very precise thermal control. Despite its limited resolution at the wavelength of the light source, optical microscopy provides a simple but practical method for studying the in situ formation of a gel superstructure on the micrometer scale. Indeed, many gels present the microstructure which can be visualized by optical microscopy,[10,11,13,15−18] although the formation of a gel network inevitably starts from self-assembly processes[19] on the molecular level (i.e., nanometer scale). An understanding of the gel structure at different scales (or levels) not only provides us with the opportunity to discuss in more detail the gelation mechanism but also sheds light on the origin of the macroscopic properties, since the microstructure of a gel network is found to be closely correlated to the mechanical and rheological properties of the gel.[15]

As is already known, the gelation of LMOGs is affected by several factors such as gelator structure,[1,3,4] solvent polarity,[1,20,21] gelator concentration,[8,18] and gelation temperature.[13] For a given gelling system, the last two factors can be described by the supersaturation in the solution (see eq 1 below). It is widely accepted that supersaturation is the dynamic driving force for gelation kinetics; however, how the supersaturation affects the formation of a fiber network, particularly the creation of the junctions, remains poor understood.

This study presents an in situ investigation of how a gel network microstructure develops in the gelation process. The

* To whom correspondence should be addressed. Telephone: +65-68742812. Fax: +65-67776126. E-mail: phyliuxy@nus.edu.sg.

10.1021/jp054531r CCC: $33.50
Published on Web 03/18/2006

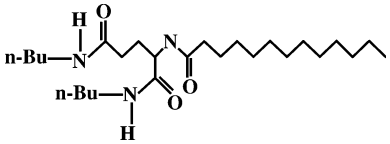

Figure 1. Chemical structure of *N*-lauroyl-L-glutamic acid di-*n*-butylamide.

role of supersaturation in the topology of a gel network and in the creation of junctions was verified. The method that regulates the supersaturation condition at the initial stage of the gelation process was proposed in an effort to obtain tunable topological structure of the gel network for a given gelling system. Finally, the correlation between the microstructure topology of a gel network and its rheological property was examined.

The gelator molecule *N*-lauroyl-L-glutamic acid di-*n*-butylamide (GP-1) used here is an amino acid-type gelator, whose chemical structure is shown in Figure 1. Its self-organized fiber network within biocompatible organic solvents such as propylene glycol (PG) or isostearyl alcohol (ISA) can be used as a novel drug carrier in transdermal drug delivery.[22] Studies seeking to control the drug release from the organogel have suggested that drug release occurs by simple diffusion.[23−25] Therefore, the topological structure of gel network is intimately involved in determining the rate of drug release. Our study would be useful for the design of GP-1/PG drug carriers with a controlled drug release rate.

2. Experimental Section

The gelling system, comprising the LMOG molecule *N*-lauroyl-L-glutamic acid di-*n*-butylamide (>98%, from Aijnomoto) and the solvent propylene glycol (>99%, Cognis), was utilized as the model to study the microstructural evolution in the gelation process. The resultant gel is normally turbid, and the microstructure can be visualized by optical microscopy. To obtain the phase diagram of the GP-1/PG system, the measurement of GP-1 solubility in PG was conducted as follows. Gels at a series of concentrations (X_{eq}) in the range from 2 to 6 wt % were prepared in glass tubes and put in a water bath. The temperature at which the last tiny part of the gel was completely dissolved was taken to be the equilibrium temperature T_{eq}. To improve the accuracy of the measurements, in the neighborhood of the equilibrium temperature, the temperature was increased in 0.2 °C increments, with 30 min between the steps.

For the optical observation, the sample films were prepared by sealing the hot GP1/PG solution in the glass cells with a spacer thickness of 0.1 mm. A conventional microscope (Olympus BX50) with a heating/cooling temperature controller (Linkam Scientific Instrument, THMS600) at the sample stage was used. The temperature ramp can be varied from 0.01 to 50 °C/min with an accuracy of 0.1 °C. The sol-to-gel transition was monitored by a microscope video system. The images from the microscope were converted to digital images through a JVC KY-F55B 3-CCD color video camera. A series of transient images were obtained during the gelation process and analyzed by the acquired image processing software (analySIS version 3.2).

Rheological experiments were performed on an advanced rheological expansion system (ARES-LS, Rheometric Scientific) equipped with 25 mm diameter parallel plate geometry. The GP1/PG gel samples were sandwiched between the two plates with a gap of 0.65 mm. To examine the mechanical properties of the GP-1/PG gels with different topological structures, a thermal control identical to that in the optical observations was followed in the rheological measurements. The time sweep experiments were performed to monitor the dynamic viscoelastic moduli during the sol-to-gel transition. The strain and frequency were set to 0.05% and 1 Hz, respectively, to prevent any major disturbance of the oscillatory shear force on the gelation process. The strain sweep was conducted to examine the critical strain at which the gel network was ruptured.

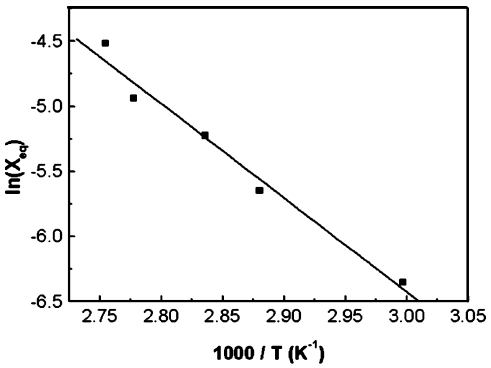

Figure 2. Plot of ln(molar fraction) vs the reciprocal of the dissolution temperature for the GP-1/PG system. The data in this phase diagram were obtained by the method described in the text. The line is the linear fit of data to extract the thermodynamic parameters according to eq 2.

3. Results and Discussion

In general, a physical organogel is formed by quenching the hot solution (sol state) of the gelling system below the gelation temperature. In this process, supersaturation is the thermodynamic driving force for the gelation kinetics. The supersaturation σ is defined as

$$\sigma(T) = \frac{X - X_{eq}(T)}{X_{eq}(T)} \tag{1}$$

where X and $X_{eq}(T)$ are the actual molar fraction and the equilibrium molar fraction of solute in solution at temperature T, respectively. The solubility, i.e., X_{eq}, for an ideal solution at a given temperature can be expressed by the van der Hoff equation:

$$\ln(X_{eq}) = -\frac{\Delta H_{diss}}{RT_{eq}} + \frac{\Delta S_{diss}}{R} \tag{2}$$

where R is the gas constant, ΔH_{diss} and ΔS_{diss} denote the molar dissolution enthalpy and the molar dissolution entropy of the nucleation phase, respectively, and T_{eq} is the equilibrium temperature for the system at a given concentration. From the phase diagram of the GP-1/PG system, the thermodynamic parameter ΔH_{diss} (~59.3 kJ/mol) was obtained by plotting ln(X_{eq}) versus $1/T_{eq}$ (Figure 2). For a given gelling process, assuming that the depletion of the solute in the solution can be neglected at the initial stage of the gelation process, the thermodynamic driving force merely varies with the temperature of the solution: as T decreases, the degree of supersaturation in the saturated solution increases. In this way, the degree of supersaturation {here $\ln[1 + \sigma(T)]$ is used} obtained from eqs 1 and 2 was taken to describe the thermodynamic driving force at the initial stage of the gelation process, and this description of the supersaturation is used throughout this paper.

For the gelation of GP-1 in PG with the concentration ranging from 2 to 6 wt %, two typical topological structures of the gel network, namely, the spherulitic network and the fibrillar network, are usually seen. The dynamic processes to form these

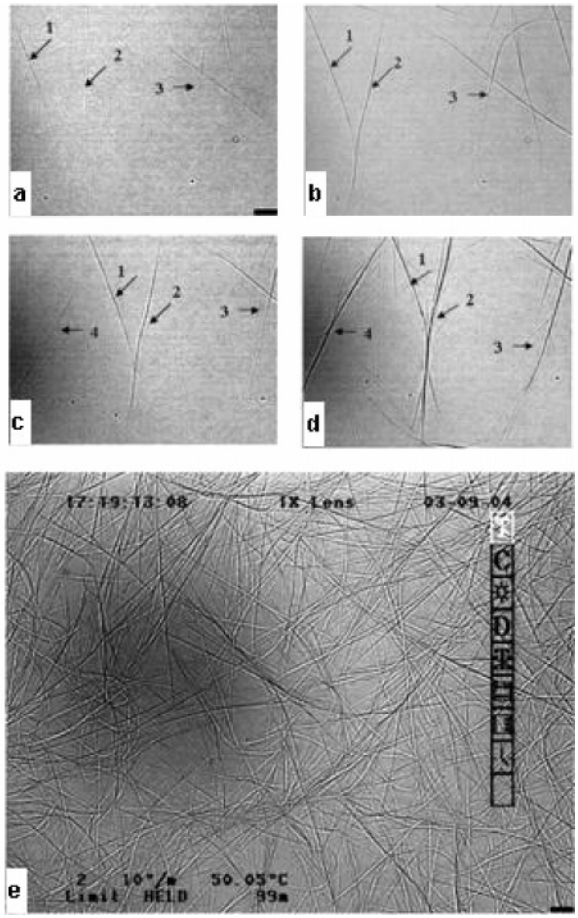

Figure 3. Micrographs showing the time evolution of the fibrillar network in the gelation process of the 2 wt % GP-1/PG system. The time zero frame was taken at the moment when the first fiber became visible in the monitored area. One-dimensional growth of the fibers was clearly seen at the beginning when cooling the solution from (a) 69.71 °C (t = 3 s) to (b) 68.68 °C (t = 9.6 s). Side branching of the fibers were seen when cooling the solution further from (c) 68.52 °C (t = 10.1 s) to (d) 67.46 °C (t = 16.6 s). (e) Fibrillar network microstructure at the final stage. The scale bar is 20 μm.

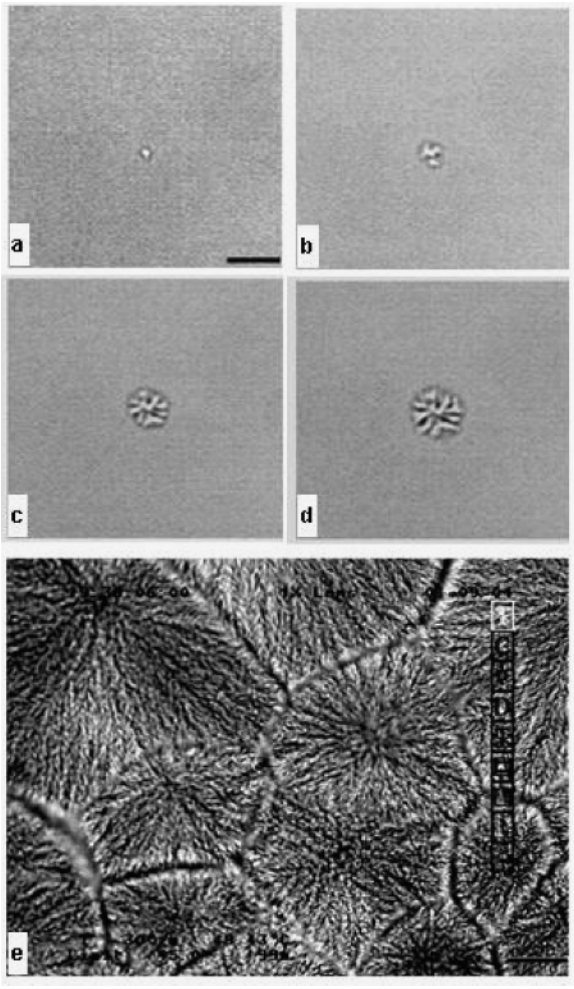

Figure 4. Micrographs showing the time evolution of the spherulitic network in the gelation process of the 6 wt % GP-1/PG system. The time zero frame was taken at the moment when the center nucleation sites became visible in the monitored area. (a) A center site at 55.05 °C (t = 0 s). (b) The needle growth at 54.97 °C (t = 0.1 s). (c) Initiation of branching on the tips of the growing fibers at 54.88 °C (t = 0.3 s). (d) Further fiber growth and tip branching at 54.77 °C (t = 0.5 s). (e) Spherulitic network microstructure at the final stage. The scale bar is 50 μm.

two typical topological structures were monitored by optical microscopy during the gelation processes.

3.1. Growth of the Fibrillar Network. The dynamic process to form the fibrillar network is shown in Figure 3, by using the 2 wt % GP-1/PG gelling system. The sample film (gel state) was heated to above the melting temperature to obtain a homogeneous solution (sol state, here T_{sol} = 80 °C), and then the solution was cooled to 50 °C at a cooling rate of 10 °C/min.

Figure 3a−d shows the growth and branching of fibers at the initial stage of gelation. At the beginning, thin fibers were observed growing in a one-dimensional way, where the degree of supersaturation was ∼0.18 (corresponding to a solution temperature of ∼70 °C). Two isolated fibers, fibers 1 and 2 (Figure 3a), were seen growing up and finally forming a transient association (Figure 3b). At the same time, fiber 3 (Figure 3a) grew up and crossed over with three other fibers (Figure 3b). Further cooling gave rise to fiber branching, as illustrated in panels c and d of Figure 3. On the side surface of fibers 1−4, branching of new fibers was clearly seen. The degree of supersaturation at which branching occurred was estimated to be 0.26 (corresponding to a solution temperature of ∼67.5 °C). Figure 3e shows the final fibrillar network microstructure in which the fibers become entangled and penetrate each other throughout the entire network. The fiber entanglements and the branching sites can be the junctions of the gel network, the former being the transient associations and the latter being the physically permanent nodes.

3.2. Growth of the Spherulitic Network. A typical process of forming the spherulitic network is shown in Figure 4. The 6 wt % GP-1/PG sample film (gel state) was heated to above the melting temperature to obtain a homogeneous solution (sol state, here T_{sol} = 110 °C), and then the solution was cooled to 45 °C at a cooling rate of 30 °C/min. Figure 4a−d shows the growth process for one of the spherulitic components in the center region of Figure 4e. At a degree of supersaturation of ∼2.07 (corresponding to a solution temperature of ∼57 °C), a center nucleation site became visible (Figure 4a). After 0.1 s, the needlelike fibers were seen growing from that nucleation site (Figure 4b). The successive images (Figure 4b−d) taken at time intervals of 0.2 s show the development of fiber branching and growth. It can be seen that branching occurred mainly on the tips of the growing fibers. Fiber growth and fiber tip branching alternated, giving rise to the formation of the treelike branching morphology of a fiber network, namely the spherulitic network.

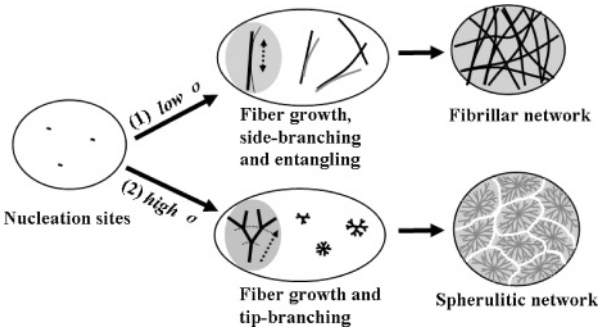

Figure 5. Two growth models of formation of a gel network. (1) Under a low degree of supersaturation to form the fibrillar network. (2) Under a high degree of supersaturation to form spherulitic network. Dashed arrows denote the growth direction of fibers, and dotted lines denote the growth front surface of the spherulite.

From the video recording, the development of the entire gel network microstructure was clearly seen. Starting from the stochastic formation of the nucleation sites, each spherulite emanated radially from the central nucleation site, and the space-filling structure was created as a consequence of the cascade of fiber branching. The advancing growth looked like a propagating wave extending from each center site to the surrounding medium radially until the neighboring spherulites impinge upon one another. Figure 4e shows the final microstructure of the gel network that consists of the microdomains of the spherulitic network. Two kinds of junction modes at the microscopic level can be clearly distinguished in the spherulitic network: the center nucleation sites of each spherulite and the branching sites in the radial arms are the permanent junctions, while the junctions that lie at the boundary between the neighboring microdomains may be the transient ones.

3.3. Supersaturation-Dependent Construction of a Gel Network. The dynamic processes shown in Figures 3 and 4 reveal two different growth models for formation of a gel network. As schematically shown in Figure 5, starting from the nucleation sites, (1) under low-supersaturation conditions, the growth of fewer-branched fibers is favored. Initiated by the entanglement and side branching of the growing fibers, the interconnected fibrillar network is built up, and (2) under high-supersaturation condition, the growth of highly branched fibers is favored and the successive branching at the growth front of the fibers develops a space-filling network structure, namely the spherulitic network.

It also suggested that the supersaturation at the initial stage of gelation would play a crucial role in tuning the structure of a gel network from the fibrillar network to the spherulitic network. A systematic study of the effect of supersaturation on the gel topological structure was conducted for the GP-1/PG system with the concentration of GP-1 in the range from 2 to 6 wt %. At a low degree of supersaturation (ranging from 0.18 to 1.5), the fibrillar network is obtained. At a degree of supersaturation of >1.5, the spherulitic network is observed.

For the development of the spherulitic network, the microstructure further shows supersaturation dependence. As shown in Figure 6, the spherulitic network microstructure formed at a degree of supersaturation of ~ 2.9 (corresponding to a gelation temperature of 35 °C) is obviously different from that formed at ~ 1.5 (corresponding to a gelation temperature of 55 °C). One can first notice that, as the degree of supersaturation increases, the spherulite size distribution decreases accordingly with the increase in the level of the spherulite components, since more nucleation sites for the spherulitic growth are stochastically formed under higher-supersaturation conditions. Moreover, with

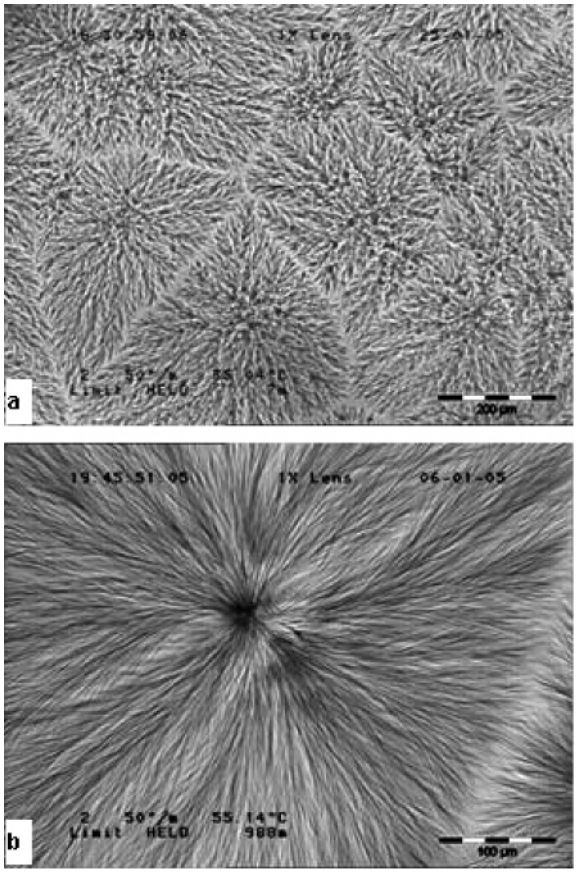

Figure 6. Micrographs of the spherulitic networks formed in the 3 wt % GP-1/PG system at (a) 35 and (b) 55 °C.

the increase in the degree of supersaturation, the average length of branches becomes shorter (or the branching frequency of the growing fibers becomes higher). In addition, our experimental results suggested that, in a certain range of gelation temperatures, the growth rate of spherulite along the radial arms varies with temperature (supersaturation); for instance, it is 0.9 μm/s at 55 °C and 1.5 μm/s at 35 °C for the 3 wt % GP-1/PG system, but the topological structure of the spherulitic network is reserved.

Considering that the cooling rate could be another important factor affecting the topological structure of a gel network, we further examined the role of the cooling rate in the topology of the GP-1/PG gel network. A series of experiments were carried out as the cooling rate changed from 50 to 5 °C/min while other experimental conditions (e.g., the initial and final temperature) were kept unchanged. The optical micrographs do not exhibit significant changes in the topological structure of the gel network. We thereby concluded that, for altering the topological structure of a gel network, the cooling rate does not have a significant influence as does the supersaturation condition at the initial stage of the gelation process.

3.4. Supersaturation-Dependent Junction Creation. It is worth noting that the creation of the junctions, in particular, the physically permanent junctions, exhibits an obvious supersaturation dependence. For a better understanding, the branching behaviors revealed in Figures 3 and 4 are schematically illustrated in Figure 5 (the middle column). At a low degree of supersaturation, the side branching of the growing fibers makes the contribution to the permanent junctions in the fibrillar network, whereas at a higher degree of supersaturation, the tip branching made a predominant contribution to the permanent junctions in the spherulitic network.

This supersaturation-dependent branching behavior can be understood in terms of the supersaturation-driven structural mismatch nucleation and growth at the interface of the growing crystal, which is called crystallographic mismatch nucleation[26−29] hereafter. The branching either on the side surface or at the tip of a growing fiber originates from this secondary nucleation at the growing crystal. Similar to normal nucleation and growth, the kinetics of crystallographic mismatch nucleation and growth depend on the degree of supersaturation at the surface of the growing crystal (called surface supersaturation hereafter), which increases monotonically with the bulk supersaturation in the system. At very low degree of bulk supersaturation, the crystallographic mismatch nucleation barrier (ΔG^*) is very high. Nucleation is governed by a process dominated by an optimal structural match and a strong interaction between the parent crystal and the newly nucleating phase.[27,28] Fiber growth without branching is favored (as shown in Figure 3a,b). As the degree of supersaturation increases, the ΔG^* will drop rapidly, and the interface structural match between the substrate and the nucleating phase will deviate from the optimal structural match position.[28,29] Once crystallographic mismatch nucleation and growth have occurred, the new-born crystal will then take an orientation which differs from that of the parent crystal,[26] leading to the appearance of a branch at the surface of the parent crystal. Surface supersaturation of a growing crystal can be the principle factor governing the branching behavior. For a fiber growing one-dimensionally, the side faces with slow integration kinetics can take advantage of the highest possible degree of supersaturation,[27] the bulk supersaturation of the system. It means that the crystallographic mismatch nucleation would be favored at the side surface. At a very high degree of supersaturation, the growth kinetics of crystal are governed by the diffusion of growth units in the viscous medium.[30,31] It is likely that the pronounced heterogeneity[32] of the viscous medium gives rise to crystallographic mismatch nucleation at the growth front, leading to spherulitic polycrystalline growth. With this polycrystalline growth mechanism, it is anticipated that branching would occur at the fiber tips which are located at the growth front surface for exposure to the high-bulk supersaturation environment. We believe that the supersaturation-driven branching behaviors described above might play an important role in the initiation and construction of a gel superstructure.[5]

3.5. Tuning the Topological Microstructure of the Gel Network To Modify the Rheological Properties. It is obvious that the topological structure is significantly different in the fibrillar network and the spherulitic network. The former (Figure 3e) is composed of fewer branched fibers entangled with each other in a disorderly manner. The interconnection of fibers extends throughout the entire network via interpenetration and entanglements. In contrast, the latter (Figure 4e) consists of two levels of networks, the first being the spherulitic domain that is highly branched fibers interconnected physically through the junctions (e.g., the center nucleation sites) and arranged radially in an orderly manner and the second being the network of spherulitic domains, between which interlinking at the boundaries may be transient compared to the permanent junctions in each spherulitic domain.

A gel with the two different topological microstructures described above would present a different rheological property. The rheological property of the gel with the fibrillar network structure depends on the distribution of junctions and the thickness and density of fibers,[15] but the rheological property of the spherulitic network would be determined mainly by the interlinking between domains. As the interlinking between domains might be very weak, it is anticipated that a weaker rheological property would be exhibited in this case. Tuning the topological structure of gel network can be the way to engineer the macroscopic property of a gel material.

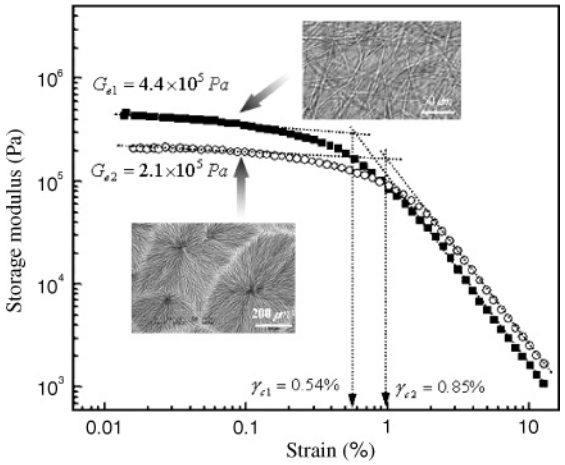

Figure 7. Strain sweep of the 3 wt % GP-1/PG gels, together with the corresponding optical micrographs. G_e denotes the plateau value of the storage modulus, and γ_c denotes the critical strain.

To emphasize the effect of tuning the topological structure on the mechanical property of a gel network, the fibrillar network and the spherulitic network were obtained separately in a given gelling system (here a 3 wt % GP-1/PG system is used), and their rheological property were examined at identical final temperatures. In this way, the total fiber mass in each gel network can be regarded as being constant, regardless of its topological structure.

We applied here a smart thermal control, which regulates not only the quenched solution temperature as in most ordinary gelation experiments but also the solution temperature at the beginning of the sol-to-gel transition. In such a way, the supersaturation at the initial stage of the gelation can be well tuned to produce a variety of gel networks. To form the fibrillar network, the thermal control was conducted from a T_{sol} of 77 °C to a T_{gel} of 50 °C with a cooling rate of 10 °C/min. To form the spherulitic network, the thermal control was conduced from a T_{sol} of 90 °C to a T_{gel} of 50 °C with a cooling rate of 10 °C/min. The degree of supersaturation at the initial stage of the gelation were estimated to be 1.1 for the fibrillar network and 1.8 for the spherulitic network.

Figure 7 shows the measurements of the rheological properties for the 3 wt % GP-1/PG gels with the fibrillar network and the spherulitic network. The plateau of the storage modulus G_e and the critical strain γ_c are 4.4×10^5 Pa and 0.54% for the gel with the fibrillar network and 2.1×10^5 Pa and 0.85% for the gel with the spherulitic network, respectively. It is concluded that the 3 wt % GP-1/PG gel has experienced a 2-fold enhancement in the storage modulus, by tuning the gel microstructure from the spherulitic network to the fibrillar network.

The fibrillar network restores a greater elastic modulus, and this network breakage at relatively small strain is probably due to the stress-induced unbinding at the entanglements. In contrast, the spherulitic network possesses less rigidity due to the weak interlinking at the boundaries which could make the slip between the neighboring spherulitic components easily. In addition, the breakage of the spherulitic network at a larger strain may suggest that the weaker junctions at the boundaries could be stronger than the entanglements of the fibrillar network. In a word, these results demonstrate that tuning the topological structure of the

GP-1/PG gel network can lead to a marked modification of its rheological properties.

4. Conclusions

Our study has demonstrated that supersaturation plays a crucial role in the topological structure of a gel network and in the creation of junctions. Thereby, we have proposed a method for tuning the topology of a gel network microstructure by regulating the supersaturation condition at the initial stage of the gelation process. This work may provide a novel approach to manipulating the formation of a molecular gel superstructure and consequently to engineering the macroscopic properties of a gel functional material.

Acknowledgment. We thank Dr. J. Narayanan and Dr. C. Strom for their valuable discussion and kind assistance.

References and Notes

(1) Terech, P.; Weiss, R. G. *Chem. Rev.* **1997**, *97*, 3133.
(2) Van Esch, J.; Schoonbeek, F.; De Loos, M.; Veen, E. M.; Kellogg, R. M.; Feringa, B. L. *NATO ASI Ser., Ser. C* **1999**, *527*, 233.
(3) Abdallah, D. J.; Weiss, R. G. *Adv. Mater.* **2000**, *12*, 1237.
(4) Gronwald, O.; Snip, E.; Shinkai, S. *Curr. Opin. Colloid Interface Sci.* **2002**, *7*, 148.
(5) Liu, X. Y.; Sawant, P. D. *Adv. Mater.* **2002**, *14*, 421.
(6) Lin, Y.; Kachar, B.; Weiss, R. G. *J. Am. Chem. Soc.* **1989**, *111*, 5542.
(7) Brotin, T.; Desvergne, J. P.; Fages, F.; Utermohlen, R.; Bonneau, R.; Bouas-Laurent, H. *Photochem. Photobiol.* **1992**, *55*, 349.
(8) Wang, R.; Geiger, C.; Chen, L.; Swanson, B.; Whitten, D. G. *J. Am. Chem. Soc.* **2000**, *122*, 2399.
(9) Geiger, C.; Stanescu, M.; Chen, L.; Whitten, D. G. *Langmuir* **1999**, *15*, 2241.
(10) Samuel, R. E.; Salmon, E. D.; Briehl, R. W. *Nature* **1990**, *345*, 833.
(11) Lescanne, M.; Colin, A.; Mondain-Monval, O.; Fages, F.; Pozzo, J.-L. *Langmuir* **2003**, *19*, 2013.
(12) Chou, C. M.; Hong, P. D. *Macromolecules* **2004**, *37*, 5596.
(13) Huang, X.; Terech, P.; Raghavan, S. R.; Weiss, R. G. *J. Am. Chem. Soc.* **2005**, *127*, 4336.
(14) Liu, X. Y.; Sawant, P. D. *Appl. Phys. Lett.* **2001**, *79*, 3518.
(15) Shin, J. H.; Gardel, M. L.; Mahadevan, L.; Matsudaira, P.; Weitz, D. A. *Proc. Natl. Acad. Sci. U.S.A.* **2004**, *101*, 9636.
(16) Ilzhoefer, J. R.; Broom, B. C.; Nepa, S. M.; Vogler, E. A.; Khan, S. A.; Spontak, R. J. *J. Phys. Chem.* **1995**, *99*, 12069.
(17) Mercurio, D. J.; Spontak, R. J. *J. Phys. Chem. B* **2001**, *105*, 2091.
(18) Kobayashi, T.; Takanaka, M.; Saijo, K.; Hashimoto, T. J. *Colloid Interface Sci.* **2003**, *262*, 456.
(19) Aggeli, A.; Nyrkova, I. A.; Bell, M.; Harding, R.; Carrick, L.; McLeish, T. C. B.; Semenov, A. N.; Boden, N. *Proc. Natl. Acad. Sci. U.S.A.* **2001**, *98*, 11857.
(20) George, M.; Snyder, S. L.; Terech, P.; Glinka, C. J.; Weiss, R. G. *J. Am. Chem. Soc.* **2003**, *125*, 10275.
(21) Geiger, C.; Stanescu, M.; Chen, L.; Whitten, D. G. *Langmuir* **1999**, *15*, 2241.
(22) (a) Kang, L. F.; Sawant, P. D.; Liu, X. Y.; Chan, S. Y. Transdermal Drug Delivery Composition Comprising A Small Molecule Gel And Process For The Preparation Thereof. U.S. Patent Appl. 79612-62, 2005. (b) Kang, L. F.; Sawant, P. D.; Liu, X. Y.; Ho, P. C. L.; Chan, Y. W.; Chan, S. Y., SMGA Gels for the Skin Permeation of Haloperidol. *J. Controlled Release* **2005** (in press).
(23) Friggeri, A.; Feringa, B. L.; Van Esch, J. *J. Controlled Release* **2004**, *97*, 241.
(24) Kantaria, S.; Rees, G. D.; Lawrence, M. J. *J. Controlled Release* **1999**, *60*, 355.
(25) Penzes, T.; Csoka, I.; Eros, I. *Rheologica Acta* **2004**, *43*, 457.
(26) Liu, X. Y. From molecular structure of solid-fluid interfaces to nucleation and growth kinetics: Implications for nanostructure engineering. In *Nanoscale structure and assembly at solid-fluid interfaces*; Liu, X. Y., De Yoreo, J. J., Eds.; Plenum/Kluwer Academic Publishers: Dordrecht, The Netherlands, 2004; Vol. 1, Chapter 5.
(27) Chernov, A. A. *Modern Crystallography III: Crystal Growth*, Springer-Verlag, Berlin, 1984.
(28) Bennema, P. *J. Cryst. Growth* **1984**, *69*, 182.
(29) Bennema, P.; Liu, X. Y.; Lewtas, K.; Tack, R. D.; Rijpkema, J. J. M.; Roberts, K. J. *J. Cryst. Growth* **1992**, *121*, 679.
(30) Storm, C. S.; Liu, X. Y.; Wang, M. *J. Phys. Chem. B* **2000**, *104*, 9638.
(31) Ben-Jacob, E.; Deutscher, G.; Garik, P.; Goldenfeld, N. D.; Lareah, Y. *Phys. Rev. Lett.* **1986**, *57*, 1903.
(32) Gránásy, L.; Pusztai, T.; Börzsönyi, T.; Warren, J. A.; Douglas, J. F. *Nat. Mater.* **2004**, *3*, 645.